

## Supporting Information

# Optimizing the growth of vertically aligned carbon nanotubes by literature mining and high-throughput experiments

Zhang-Dan Gao<sup>1,2,†</sup>, Zhong-Hai Ji<sup>1,2,†</sup>, Lili Zhang<sup>1,\*</sup>, Dai-Ming Tang<sup>3,\*</sup>, Meng-Ke Zou<sup>1,2</sup>, Rui-Hong Xie<sup>1,2</sup>, Shao-Kang Liu<sup>1,2</sup>, Chang Liu<sup>1,\*</sup>

<sup>1</sup>Shenyang National Laboratory for Materials Science, Institute of Metal Research (IMR), Chinese Academy of Sciences, Shenyang 110016, China;

<sup>2</sup>School of Materials Science and Engineering, University of Science and Technology of China, Hefei 230026, China;

<sup>3</sup>Research Center for Materials Nanoarchitectonics (MANA), National Institute for Materials Science (NIMS), Tsukuba, Ibaraki 305-0044, Japan

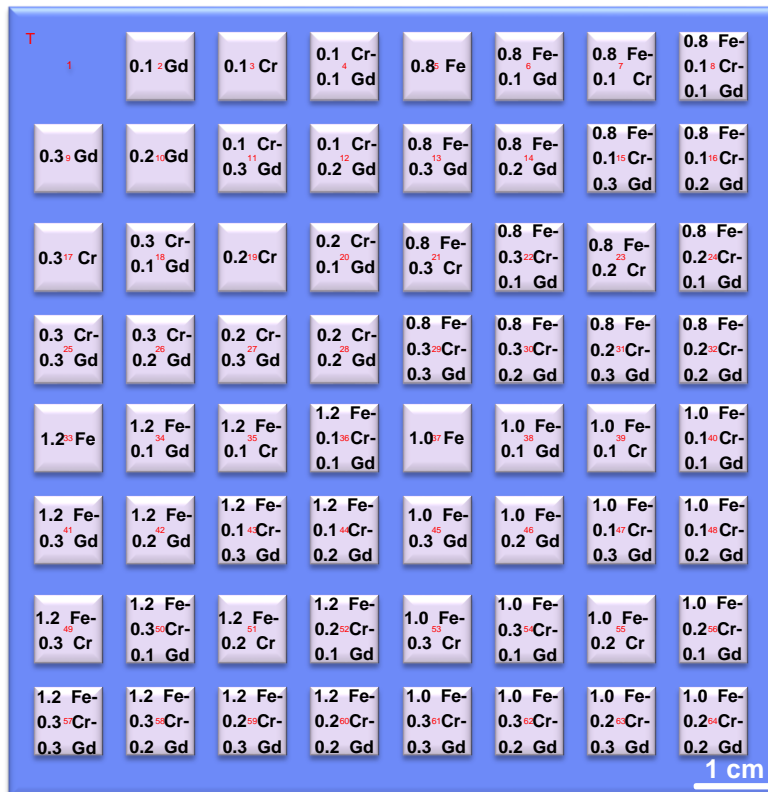


Figure S1. Schematic diagram of the nominal thickness of the Fe-Cr-Gd ternary catalyst library obtained using the combined masking method. The values of  $t_{\text{Cr}}$  and  $t_{\text{Gd}}$  are from 0 to 0.3 nm and the values of  $t_{\text{Fe}}$  are from 0 to 1.2 nm. The red numbers from 1 to 64 represent the marks on the silicon wafer.

Table S1. Statistical classification of manual data mining results.

| Input parameter       |                               |                               |                                  |                  |                   |                                 |   |
|-----------------------|-------------------------------|-------------------------------|----------------------------------|------------------|-------------------|---------------------------------|---|
| Annealing temperature | Annealing atmosphere          |                               |                                  | Primary catalyst | Co-catalyst       | Support layer                   | Annealing time                                  |
| /                     | H <sub>2</sub>                | Ar                            | C <sub>2</sub> H <sub>2</sub>    | ...              | Fe Co             | Gd                              | Al <sub>2</sub> O <sub>3</sub> SiO <sub>2</sub> |
| Growth temperature    | Carbon source                 |                               |                                  | Growth promoter  | Carrier gas       |                                 | Growth time                                     |
| /                     | C <sub>2</sub> H <sub>2</sub> | C <sub>2</sub> H <sub>4</sub> | C <sub>2</sub> H <sub>5</sub> OH | ...              | Ar H <sub>2</sub> | O <sub>2</sub> H <sub>2</sub> O | ...   |
| Output parameter      |                               |                               |                                  |                  |                   |                                 |   |
| Height                |                               |                               |                                  | $I_G/I_D$ value  |                   |                                 |   |

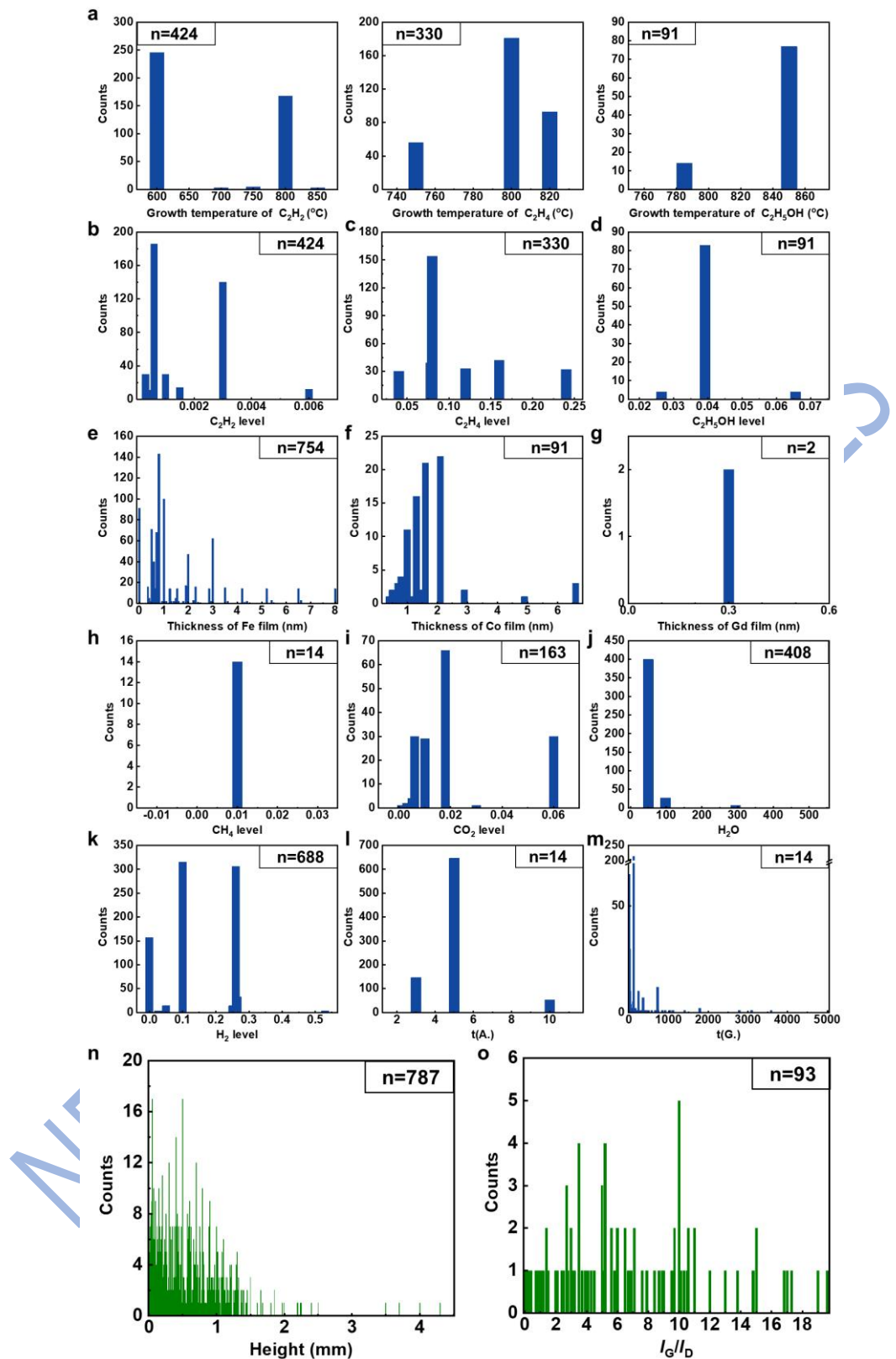


Figure S2. Distribution of 13 growth parameters (a-m) and 2 structural data (n-o) in the literature investigation. (a) Demonstrates the growth temperature distribution of  $\text{C}_2\text{H}_2$ ,  $\text{C}_2\text{H}_4$ ,  $\text{C}_2\text{H}_5\text{OH}$ . n denotes the number of recipes.

Table S2. Optimized hyperparameters for random forest regression (RFR) and support vector regression (SVR) on the training data for different output parameters. A grid search method was used to obtain the listed values for optimizing the structure of the machine learning models.

| Output parameters | Hyperparameter |                 |                      |
|-------------------|----------------|-----------------|----------------------|
|                   | RFR            | SVR             |                      |
|                   |                | Number of trees | Penalty parameter C) |
| Height            | 50             | 200             | 500                  |
| $I_G/I_D$         | 70             | 20              | 1                    |

Table S3. Average k-fold cross-validation (CV) scores for prediction height (10-fold) and  $I_G/I_D$  values (5-fold) using 3 different machine learning models.

| Output parameters | CV score |      |      |
|-------------------|----------|------|------|
|                   | LR       | RFR  | SVR  |
| Height            | 0.30     | 0.73 | 0.32 |
| $I_G/I_D$         | 0.44     | 0.66 | 0.26 |

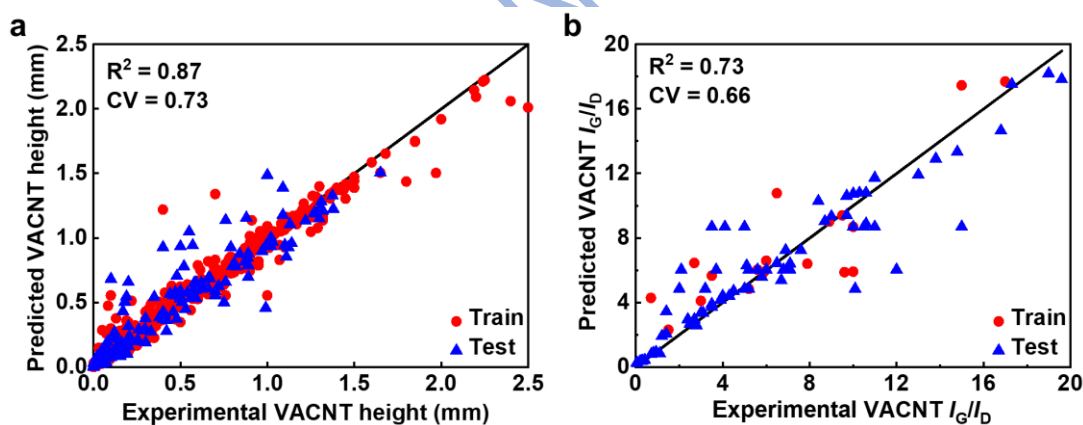


Figure S3. Linear fit between literature statistics and RFR predicted values for performance assessment of the model. (a) Height. (b)  $I_G/I_D$  values. Red circles and blue triangles represent the training and test set, respectively.

Table S4. Range and step size of growth parameters for determining the growth window for VACNTs.

| Growth parameters              | Range   | Step  |
|--------------------------------|---------|-------|
| Thickness of Fe film /nm       | 0-9.45  | 0.15  |
| Growth temperature /°C         | 750-820 | 20    |
| Carbon source concentration /% | 0-0.201 | 0.067 |

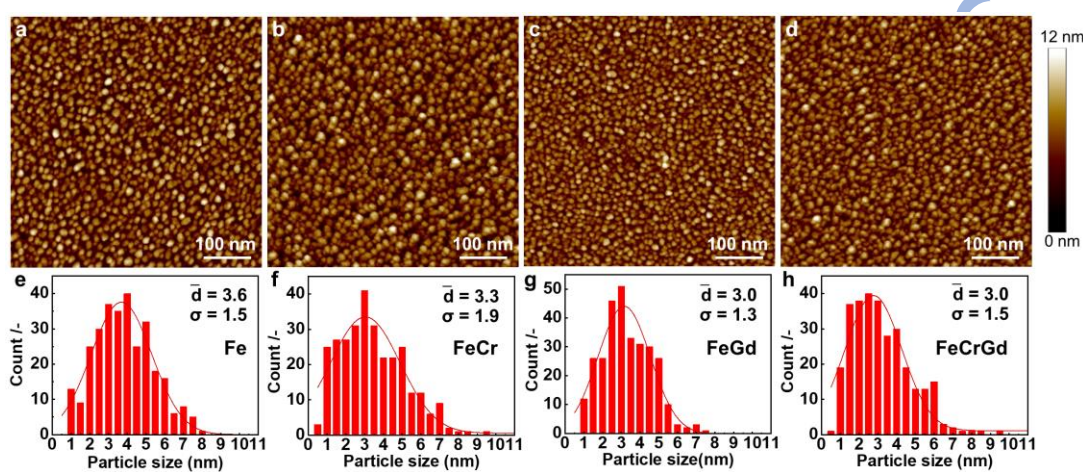
Figure S4. Average nanoparticle size and their size distribution of different catalysts on Al<sub>2</sub>O<sub>3</sub> support layer after annealing under H<sub>2</sub> and Ar at 800°C for 10 min. (a) 1.2 nm Fe. (b) 1.1 nm Fe/0.1 nm Cr. (c) 1.1 nm Fe/0.1 nm Gd. (d) 1.0 nm Fe/0.1 nm Cr/0.1 nm Gd.

Table S5. Optimized hyperparameters for random forest regression (RFR) and support vector regression (SVR) on the training data for different output parameters based on high-throughput growth experiments. A grid search method was used to obtain the listed values for optimizing the structure of the machine learning models.

| Output parameters | Hyperparameter  |                     |                    |
|-------------------|-----------------|---------------------|--------------------|
|                   | RFR             |                     | SVR                |
|                   | Number of trees | Penalty parameter C | Gamma ( $\gamma$ ) |
| Height            | 70              | 30                  | 1                  |
| $I_G/I_D$         | 60              | 200                 | 1                  |

Table S6. Average 10-fold cross-validation (CV) scores for prediction Height and  $I_G/I_D$  values using 3 different machine learning models based on high-throughput growth experiments.

| Output parameters | CV score |      |      |
|-------------------|----------|------|------|
|                   | LR       | RFR  | SVR  |
| Height            | 0.27     | 0.76 | 0.34 |
| $I_G/I_D$         | 0.36     | 0.73 | 0.18 |

Table S7. Regression model validation and performance evaluation based on high-throughput growth experiments.

| Output Parameters | Regression model | Performance evaluation metrics |      |  |
|-------------------|------------------|--------------------------------|------|--|
|                   |                  | RMSE                           | MAE  | Coefficient of Determination ( $R^2$ ) |
| Height            | LR               | 0.18                           | 0.14 | 0.29                                   |
|                   | RFR              | 0.09                           | 0.06 | 0.83                                   |
|                   | SVR              | 0.12                           | 0.09 | 0.70                                   |
| $I_G/I_D$         | LR               | 1.09                           | 0.79 | 0.32                                   |
|                   | RFR              | 0.61                           | 0.42 | 0.77                                   |
|                   | SVR              | 0.80                           | 0.49 | 0.67                                   |

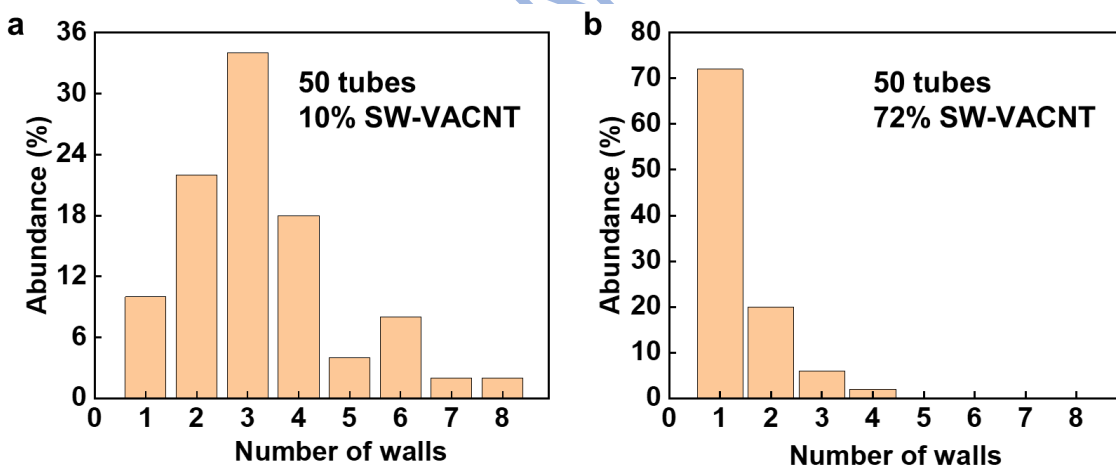


Figure S5. Wall number distributions of VACNT arrays grown from (a) 1.8 nm Fe catalyst and (b) 1.5 nm Fe/0.2 nm Gd catalyst.

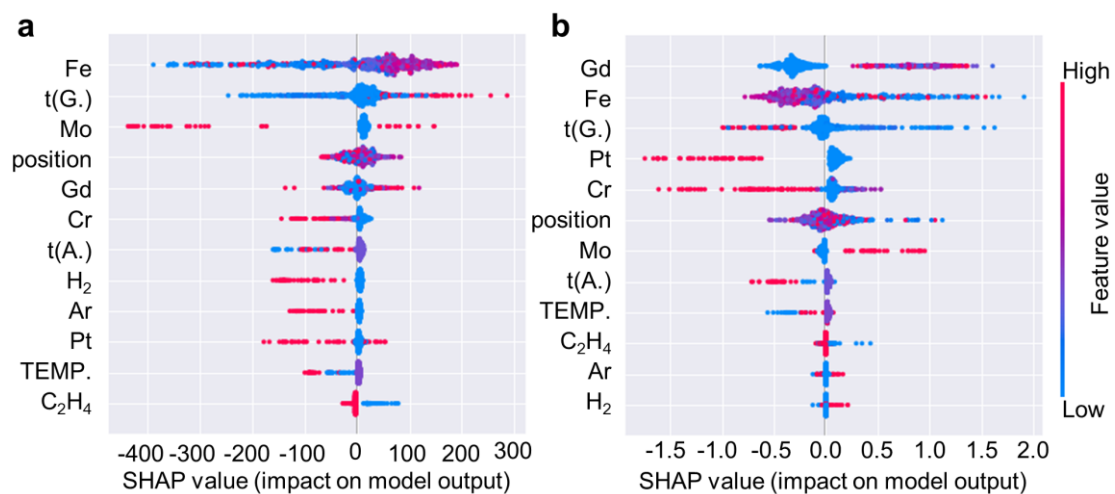


Figure S6. SHAP model for ranking the importance of growth parameters. The output parameters are height (a) and  $I_G/I_D$  value (b) of VACNTs. t(G.) and t(A.) denote the growth time and annealing time, respectively. Position indicates the coordinates of the sample in the marked silicon wafer.